The C-terminal region of A-kinase anchor protein 350 (AKAP350A) enables formation of microtubule-nucleation centers and interacts with pericentriolar proteins

Received for publication, July 7, 2017, and in revised form, October 6, 2017 Published, Papers in Press, October 20, 2017, DOI 10.1074/jbc.M117.806018

Elena Kolobova[‡§], Joseph T. Roland[‡§], Lynne A. Lapierre[‡§], Janice A. Williams[¶], Twila A. Mason[§‖], and James R. Goldenring[‡§‖1]**

*From the Departments of [‡]Surgery and [‖]Cell and Developmental Biology, the [§]Epithelial Biology Center, Vanderbilt University School of Medicine, and the **Nashville Department of Veterans Affairs Medical Center and [¶]Vanderbilt Cell Imaging Shared Resource, Nashville, Tennessee 37232*

Edited by Velia M. Fowler

Microtubules in animal cells assemble (nucleate) from both the centrosome and the cis-Golgi cisternae. A-kinase anchor protein 350 kDa (AKAP350A, also called AKAP450/CG-NAP/AKAP9) is a large scaffolding protein located at both the centrosome and Golgi apparatus. Previous findings have suggested that AKAP350 is important for microtubule dynamics at both locations, but how this scaffolding protein assembles microtubule nucleation machinery is unclear. Here, we found that overexpression of the C-terminal third of AKAP350A, enhanced GFP-AKAP350A(2691–3907), induces the formation of multiple microtubule-nucleation centers (MTNCs). Nevertheless, these induced MTNCs lacked "true" centriole proteins, such as Cep135. Mapping analysis with AKAP350A truncations demonstrated that AKAP350A contains discrete regions responsible for promoting or inhibiting the formation of multiple MTNCs. Moreover, GFP-AKAP350A (2691–3907) recruited several pericentriolar proteins to MTNCs, including γ-tubulin, pericentrin, Cep68, Cep170, and Cdk5RAP2. Proteomic analysis indicated that Cdk5RAP2 and Cep170 both interact with the microtubule nucleation-promoting region of AKAP350A, whereas Cep68 interacts with the distal C-terminal AKAP350A region. Yeast two-hybrid assays established a direct interaction of Cep170 with AKAP350A. Super-resolution and deconvolution microscopy analyses were performed to define the association of AKAP350A with centrosomes, and these studies disclosed that AKAP350A spans the bridge between centrioles, co-localizing with rootletin and Cep68 in the linker region. siRNA-mediated depletion of AKAP350A caused displacement of both Cep68 and Cep170 from the centrosome. These results suggest that AKAP350A acts as a scaffold for factors involved in microtubule nucleation at the centrosome and coordinates the assembly of protein complexes associating with the intercentriolar bridge.

Centrosomes are the major microtubule-organizing centers (MTOCs)[2] in eukaryotes. The architecture of centrosomes was revealed by electron microscopy, which determined that in human cells centriole cylinders are organized as nine triplets of microtubules (1–3). Each centrosome contains two centrioles that are surrounded by an electron-dense protein mass, designated the pericentriolar material or matrix (PCM), which appears as a cloud under the electron microscope. Centrioles are functionally asymmetrical (4, 5), and only the older "mother" centriole has subdistal appendages and therefore is capable of anchoring microtubules in interphase. Moreover, only the mother centriole can originate a primary cilium through attachment of distal appendages to plasma membrane. The mother centriole is associated with more abundant PCM (6). Recent proteomics studies of isolated centrosomes determined that PCM contains more than 100 different proteins (7, 8). Despite the amorphous appearance on electron micrographs, additional careful analysis of the spatial organization of some PCM proteins using subdiffraction imaging has revealed that the PCM has more structured organization than it was generally believed (9, 10).

The A-kinase anchoring proteins (AKAPs) were discovered as protein kinase A (PKA) anchors that establish localized cAMP/PKA signaling through sequestration of PKA, but they play many other roles in protein scaffolding (11, 12). AKAP350A/AKAP450/CG-NAP/AKAP9 is associated with both centrosomes and the Golgi apparatus (13–15) and also contributes in the stress response (16, 17). Centrosomes are the major MTOCs in eukaryotes. However, recently the role of the Golgi apparatus in microtubule nucleation has also become apparent. Nucleation of microtubules at Golgi apparatus depends on recruitment of AKAP350A by the cis-Golgi protein gm130 (18, 19). AKAP350A modulates microtubule stabil-

This work was supported by National Institutes of Health Grant R01 DK043405 (to J. R. G.). The authors declare that they have no conflicts of interest with the contents of this article. The content is solely the responsibility of the authors and does not necessarily represent the official views of the National Institutes of Health.
This article contains supplemental Figs. S1–S6, Table S1, and Videos S1–S2.
This article was selected as one of our Editors' Picks.

[1] To whom correspondence should be addressed: Epithelial Biology Center, Vanderbilt University School of Medicine, MRB IV, Rm. 10435-G, 2213 Garland Ave., Nashville, TN 37232. Tel.: 615-936-3726; Fax: 615-343-1591; E-mail: jim.goldenring@vanderbilt.edu.

[2] The abbreviations used are: MTOC, microtubule-organizing center; EGFP, enhanced GFP; MTNC, microtubule-nucleation center; PCM, pericentriolar material or matrix; CTD, centrosome targeting domain; MudPIT, multidimensional protein identification technology; 3D-SIM, three-dimensional structured illumination microscopy; PCC, Pearson's correlation coefficient; PO, propylene oxide; PFA, paraformaldehyde; γTuRC, γ-tubulin ring complex; PACT, pericentrin-AKAP450 centrosomal targeting.

ity and outgrowth from the centrosomes. The depletion of AKAP350 by siRNA delayed microtubule re-growth from the centrosome after nocodazole-induced depolymerization (20). Interestingly, depletion of AKAP350A also induced activation of cdc42 during microtubule re-growth (20). AKAP350 is critical for microtubule nucleation at the Golgi apparatus and stabilization of microtubules at the centrosome (18). Depletion of AKAP350 also led to diminished formation of the nucleus–centrosome–Golgi axis and defective cell migration (21). AKAP350 together with kendrin may support microtubule nucleation by anchoring the γ-tubulin ring complex (γTuRC) at the centrosome (22). Association of AKAP350 with the centrosome is critical for centrosome reproduction, and displacement of endogenous AKAP350 from the centrosome by overexpression of the C terminus of AKAP350 (AKAP350CTD, centrosome targeting domain) impairs centriole duplication (23). Depletion of AKAP350 also inhibits G_1/S transition and centrosome duplication (24). AKAP350 scaffolds Cdk2 to the centrosome, and AKAP350CTD increases centrosomal Cdk2 activity (24). Furthermore, overexpression of AKAP350CTD enhanced nucleophosmin phosphorylation by Cdk2 (24). All of these findings suggest that AKAP350 plays an important role in both centrosomal and Golgi microtubule dynamics.

In this study, we discovered that expression of the C-terminal third of AKAP350A induced supernumerary MTNCs, suggesting a role for AKAP350A in initiation of microtubule nucleation. We have identified distinct regions within AKAP350A that are accountable for promotion or inhibition of the creation of multiple MTNCs. Using a proteomics approach, we identified components of a centrosomal AKAP350A-scaffolded complex containing cyclin-dependent kinase 5 regulatory subunit-associated protein 2 (Cdk5RAP2), centrosomal protein 170 kDa (Cep170), and centrosomal protein 68 kDa (Cep68). Knockdown of AKAP350 expression with siRNA elicited the loss of Cep68 and Cep170 from the centrosome. Finally, through super-resolution microscopy and deconvolution microscopy, we have obtained high-resolution images of endogenous AKAP350A at the centrosome and propose a model for AKAP350A contributing to the linker that serves as a bridge between centrioles. All these studies support a role for AKAP350A as a coordinating scaffold for proteins involved in the regulation of microtubule nucleation.

Results

Synthetic construct of AKAP350A targets to the centrosome

Endogenous AKAP350A co-localizes with both the centrosome and Golgi apparatus. The length of the AKAP350A sequence makes analysis of protein function difficult. To facilitate this analysis of AKAP350 function, we synthesized the full-length coding sequence for AKAP350A in three ~4000-nucleotide fragments: AKAP350A(1–1383), AKAP350A (1384–2690), and AKAP350A(2691–3907) (designated EGFP-F1AKAP350A, EGFP-F2-AKAP350A, and EGFP-F3-AKAP350A, respectively); and we assembled them as EGFP fusions. The full-length EGFP-AKAP350A vector was transfected into HeLa cells (Fig. 1*A*) or U2OS cells (data not shown), and the fluorescent chimeric AKAP350A strongly accumulated at the centrosomes, with less apparent accumulation at the Golgi apparatus (Fig. 1*A*), demonstrating proper targeting of overexpressed EGFP-AKAP350A to the centrosome.

Overexpression of an AKAP350A truncation mutant causes formation of multiple γ-tubulin-containing units

We had previously noted that a short C-terminal truncation, AKAP350A(3642–3907), previously designated the "centrosome targeting domain" or CTD and containing the "pericentrin-AKAP450 centrosomal targeting" (PACT) domain (amino acids 3704–3786) (25) demonstrated expression at the centrosome (26). Thus, it was surprising when we observed that overexpression of an extended construct comprising the C-terminal third of AKAP350A, EGFP-AKAP350A(2691–3907), induced formation of multiple units, whereas the shorter C-terminal fragment, AKAP350A(3642–3907) or CTD, was directed to a single centrosome (Fig. 1*B*). In contrast, both EGFP-AKAP350A(1–1383) and EGFP-AKAP350A(1384–2690) demonstrated a cytosolic cell distribution (data not shown). EGFP-AKAP350A(2691–3907)-induced units were positive for both γ-tubulin (Fig. 1*B*) and pericentrin. These findings suggested that a region of AKAP350A distinct from the centrosomal targeting PACT domain regulated induction of multiple γ-tubulin-positive units. In the following discussion, we will refer to EGFP-AKAP350A(2691–3907) as EGFP-F3-AKAP350A.

Multiple units induced by expression of EGFP-F3-AKAP350A are functional MTNCs

To determine whether the multiple units caused by EGFP-F3-AKAP350A expression are functional microtubule nucleation/organization centers rather that just agglomerates of overexpressed protein pulling in γ-tubulin, we performed a nocodazole wash-out assay. We pre-treated HeLa cells with nocodazole to depolymerize microtubules and monitored recovery after removal of nocodazole. HeLa cells transfected with EGFP-F3-AKAP350A were treated with 33 μM nocodazole for 2 h at 37 °C to depolymerize microtubules, washed with DMEM, allowed to recover for 30 min to initiate microtubule recovery, fixed in methanol, and stained for α-tubulin and γ-tubulin. We observed that the multiple units induced by overexpression of EGFP-F3-AKAP350A served as centers for microtubule aster formation (Fig. 2). Thus, the AKAP350A-induced multiple units were competent MTNCs.

To evaluate the microtubule nucleation capacity of the MTNCs induced by overexpression of EGFP-F3-AKAP350A, we evaluated the time course of microtubule re-growth from centrosomal MTOCs *versus* ectopic EGFP-F3-AKAP350A-induced MTNCs following nocodazole removal. We observed that MTNC units induced by overexpression of EGFP-F3-AKAP350A varied greatly in the ability to nucleate microtubules (Fig. 3). Although a few MTNCs displayed a rate of microtubule re-growth similar to centrosomes, a significant proportion of asters originating from MTNCs were smaller than those that originated from centrosomal MTOCs. At 10 min of nocodazole recovery, the average size of microtubules nucleated at centrosomal MTOCs was 2.00 ± 0.90 μm^2 *versus* 1.43 ± 0.85 μm^2 from ectopic MTNCs ($p = 0.0001$). Similarly, after 20 min of nocodazole recovery, microtubules nucleated from centrosomes averaged 5.08 ± 3.9 μm^2 compared with

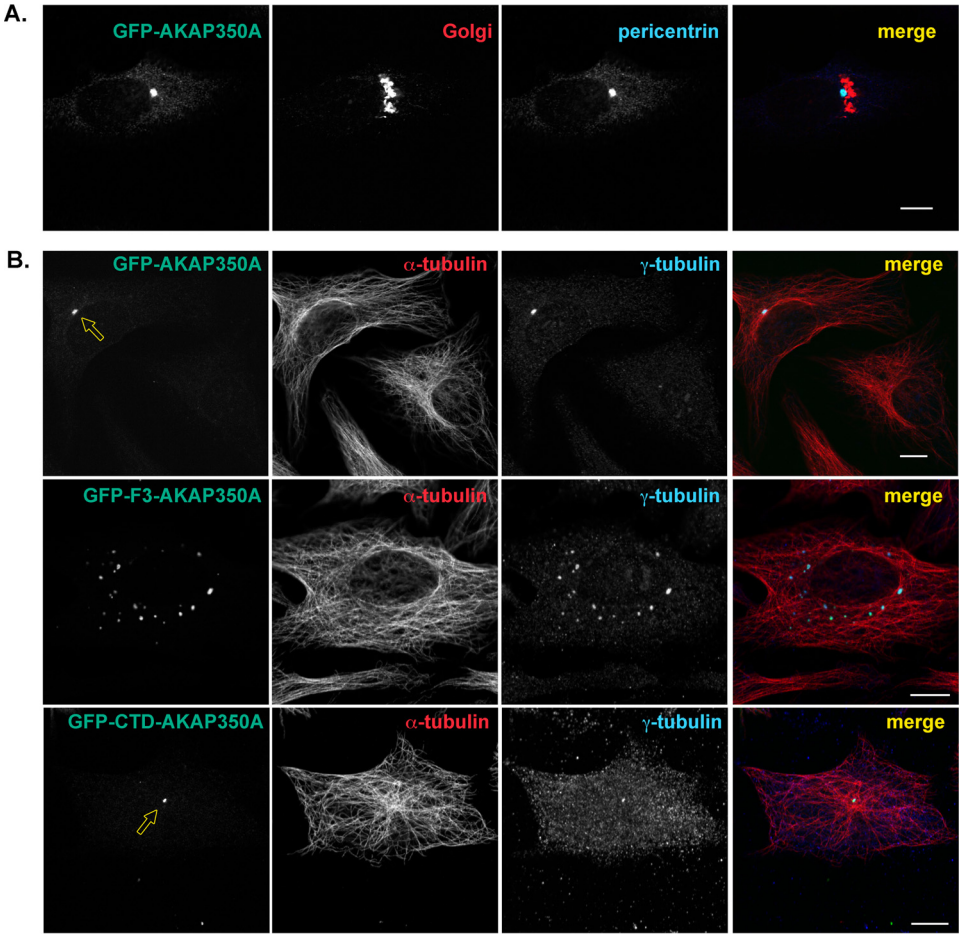

Figure 1. Distribution of overexpressed AKAP350A constructs. *A,* EGFP-AKAP350A was expressed in HeLa cells, which were stained with antibodies against the cis-Golgi protein gm130 (*red*) and the centrosome protein pericentrin (*blue*). Synthetic full-length AKAP350A was strongly accumulated at the centrosomes, with less apparent accumulation at the Golgi apparatus. *B,* HeLa cells expressing EGFP chimeras were fixed with methanol and stained for α-tubulin (*red*) and γ-tubulin (*blue*). *Open arrows* indicate single centrosomes. Overexpression of EGFP-F3-AKAP350A(2691–3907) but not EGFP-AKAP350A or EGFP-CTD-AKAP350A(3642–3907) induced formation of multiple γ-tubulin-containing units. *Bar,* 10 μm.

3.36 ± 2.43 μm^2 for microtubules nucleated from ectopic MTOCs ($p = 0.0019$). It is notable that later in nocodazole recovery, we observed a greater population of smaller MTNCs. This may suggest that MTNCs induced by overexpression of EGFP-F3-AKAP350A are sufficient for initialization of microtubule re-growth but lack some components required to maintain or stabilize microtubule re-polymerization. These results are consistent with the property of full-length AKAP350A to stabilize microtubules elongating from MTOCs (20).

Recent investigations have suggested that the cis-Golgi protein gm130 is essential for microtubule nucleation at the Golgi apparatus through recruitment of AKAP350 to nucleation sites (18). To determine whether EGFP-F3-AKAP350A-induced MTNCs originated from the Golgi apparatus, we stained HeLa cells expressing EGFP-F3-AKAP350A with an antibody against gm130. Fig. 4 demonstrates that AKAP350A-induced MTNCs are not associated with gm130-labeled cis-Golgi membranes.

De novo formation of MTNCs induced by overexpression of the C-terminal third of AKAP350A, EGFP-F3-AKAP350A

To examine the formation of MTNCs, we monitored the development of EGFP-F3-AKAP350A-induced microtubule nucleation centers in live cells. Imaging (Fig. 5 and supplemental video S1) was initiated 6 h following transfection and recorded for 80 min, every 2 min. Snapshots from the video shown in Fig. 5*A* were taken every 10 min. MTNCs induced by EGFP-F3-AKAP350A appeared to form *de novo*. Furthermore, we monitored the dynamics of newly formed MTNCs at later stages (20 h after transfection) using DeltaVision deconvolution live-cell microscopy. Imaging (Fig. 5 and supplemental video S2) was initiated 20 h after transfection and recorded for 2 h every 2 min. Snapshots of the live imaging of EGFP-F3-AKAP350A (Fig. 5*B*) show the presence of multiple donut-shaped rings.

Using high-resolution deconvolution microscopy, we demonstrated that MTNCs have a circular EGFP-F3-AKAP350A-containing structure surrounding a core of γ-tubulin (Fig. 6*A*). Evaluation of EGFP-F3-AKAP350A-induced MTNCs by transmission electron microscopy did not reveal the presence of any supernumerary centriole structures. Rather we observed only in EGFP-F3-AKAP350A-expressing cells the presence of 100–150-nm electron-dense fibrillar structures that were not present in any non-transfected cells (Fig. 6*B*).

Characterization of MTNC protein composition

To determine the characteristics of the induced MTNCs, we analyzed recruitment of various endogenous centrosomal pro-

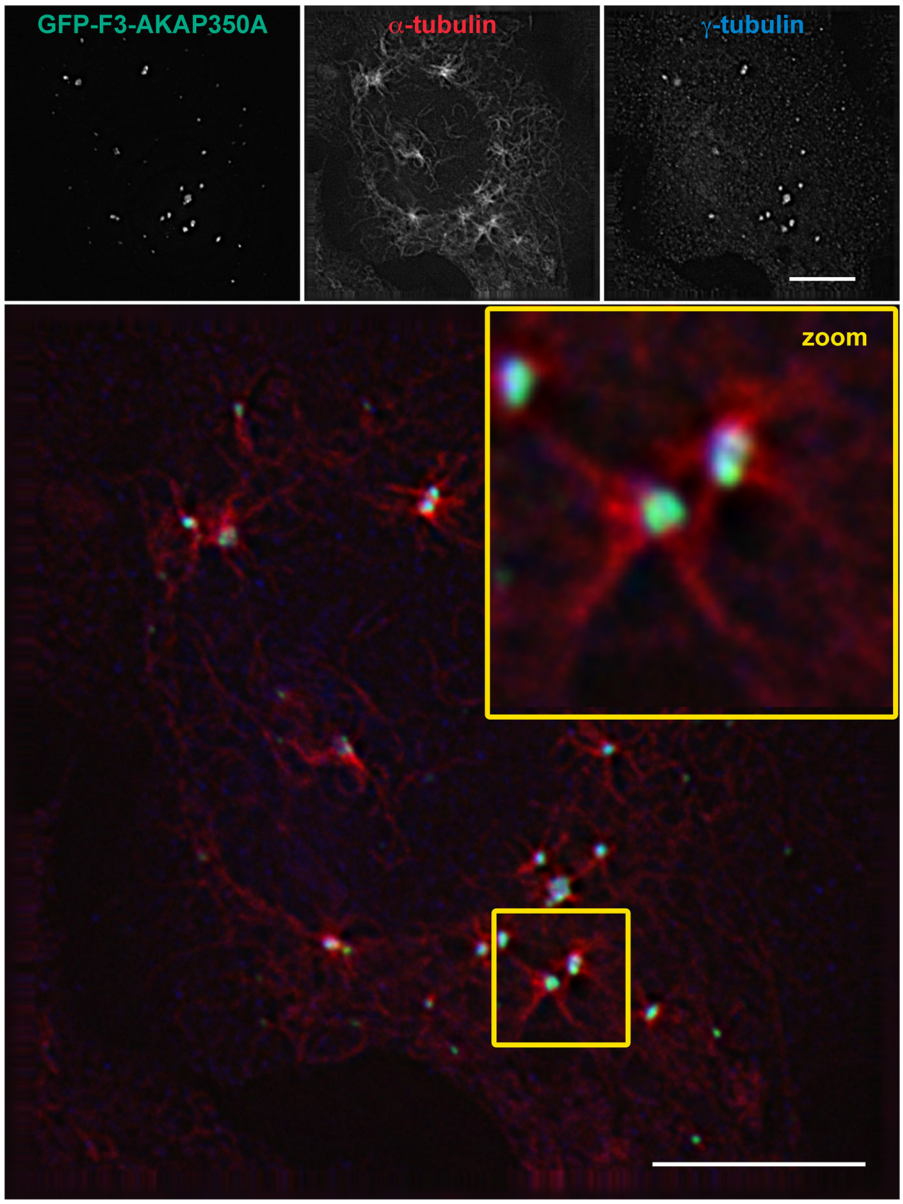

Figure 2. Induction of γ-tubulin-containing units caused by overexpression of EGFP-F3-AKAP350A are functional MTNCs. HeLa cells transfected with EGFP-F3-AKAP350A were treated with 33 μM nocodazole for 2 h at 37 °C to depolymerize microtubules, washed with DMEM, and allowed to recover for 30 min to initiate microtubule recovery, fixed in methanol, and stained for α-tubulin (*red*) and γ-tubulin (*blue*). Formation of microtubules asters originated from numerous γ-tubulin-containing units during recovery after nocodazole treatment. *Bar,* 10 μm.

teins by overexpression of EGFP-F3-AKAP350A. HeLa cells overexpressing EGFP-F3-AKAP350A were stained for endogenous γ-tubulin, pericentrin, Cep135, Cep170, Cdk5RAP2, and Cep68 (Fig. 7). We observed that EGFP-F3-350A recruited various pericentriolar proteins, including γ-tubulin, pericentrin, Cep68, Cep170, and Cdk5RAP2. Nevertheless, the MTNCs induced by overexpression of the C-terminal third of AKAP350A did not contain "true" centriolar markers, such as Cep135.

Mapping of AKAP350 regions responsible for the formation of supernumerary MTNCs

To determine the regions of AKAP350A responsible for the formation of supernumerary MTNCs, we made several truncation mutants, depicted in Fig. 8, and we assessed their cellular localization and centrosomal phenotype. As shown above, overexpression of EGFP-F3-AKAP350A led to formation of supernumerary MTNCs, whereas shorter constructs containing the CTD and the full-length AKAP350A were directed to a single centrosome. These findings suggested that regions within AKAP350A must promote or inhibit formation of multiple MTNCs.

To analyze the location of the promoting region, we expressed three truncations of EGFP-F3-AKAP350A, each removing coiled-coil regions (F3Δ1-AKAP350A, F3Δ2-AKAP350A, and F3Δ3-AKAP350A) (supplemental Fig. S1). The truncation without the first, most N-terminal coiled-coil region in F3Δ1-AKAP350A still produced multiple MTNCs, whereas removal of the second coiled-coil in F3Δ2-AKAP350A caused a mixed phenotype, with cells showing both single and multiple MTNCs. However, removal of all three coiled-coil regions (F3Δ3-AKAP350A)

restored the predominantly single centrosome localization phenotype (supplemental Fig. S1). Therefore, we defined the region between amino acids 2762 and 3458 as an MTNC "promoting region" (given that an addition of the two additional coiled-coil domains in amino acids 2762–3458 shifted the cell phenotype from regular singular centrosomes to cells showing multiple MTNCs).

Because overexpressed full-length EGFP-AKAP350A targets to the centrosome and does not cause initiation of MTNCs, we hypothesized that there should be a sequence between the N terminus of AKAP350A and amino acid 2762 that prevents formation of multiple MTNCs under normal conditions. Using further N-terminal truncation mutants, we were able to identify a change of phenotype from multiple MTNCs (with EGFP-F2F3Δ2-AKAP350A) back to a predominantly single centrosome phenotype (with EGFP-F2F3Δ1-AKAP350A) with the addition of sequence between amino acids 1882 and 2182, which we have designated as an MTNC "inhibitory region" (supplemental Fig. S2).

Importantly, dual overexpression of EGFP-tagged F2F3Δ1-AKAP350A with mCherry tagged F3-AKAP350A abolished the formation of multiple MTNCs and led to enlargement of the labeled PCM (supplemental Fig. S3) (compare with supernumerary MTNCs formed due to overexpression of EGFP-F3-AKAP350 shown in supplemental Fig. 1). These findings could suggest that the inhibitory region has a dominant capacity for preventing formation of multiple MTNCs and can act in *trans* against the promoting region. Also, intermolecular conformational changes within AKAP350A, which are regulated by the numerous cellular factors that control its activity, could lead to an inhibitory effect.

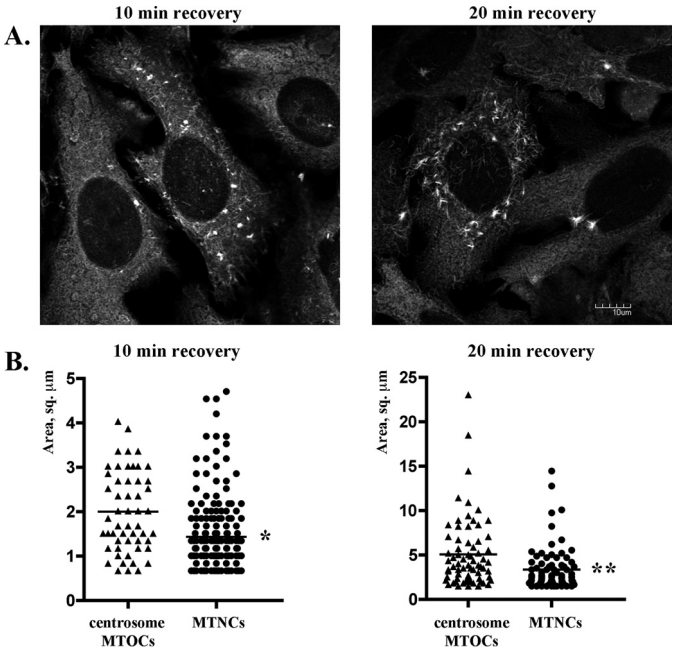

Figure 3. Comparison of centrosome MTOCs with EGFP-F3-AKAP350A-induced MTNCs. *A,* HeLa cells transfected with EGFP-F3-AKAP350A were treated with 33 μM nocodazole for 2 h at 37 °C to depolymerize microtubules, washed with DMEM, and allowed to recover for 10 or 20 min to initiate microtubule recovery, fixed in methanol, and stained for α-tubulin. *Bar,* 10 μm. *B,* formation of microtubules asters was quantified using ImageJ particle analysis. After 10 min of nocodazole recovery, the average size of asters originating from centrosome MTOCs sizes was 2.00 ± 0.90 μm^2 (n = 54) *versus* 1.43 ± 0.85 μm^2 for induced MTNCs (n = 177) (*, p = 0.0001); after 20 min of nocodazole recovery, the average centrosome MTOC aster size was 5.08 ± 3.9 μm^2 (n = 71) *versus* 3.36 ± 2.43 μm^2 for induced MTNCs (n = 79) (**, p = 0.0019). (Data are presented as average ± S.D.).

Identification of components of a centrosomal AKAP350A-scaffolded complex

Because we identified discrete regions within the C-terminal third of AKAP350A involved in either the promotion or inhibition of the formation of supernumerary MTNCs, we performed a proteomic analysis of AKAP350A-interacting proteins to identify possible mediators of AKAP350A-associated microtubule nucleation. GFP-tagged truncation mutants of AKAP350A exhibiting different phenotypes, F3Δ3(3458–3907), F3(2691–3907), and F2F3Δ1(1882–3907) as described in Fig. 8, were overexpressed in HEK cells and isolated with GFP-binding protein beads (27), and proteins were submitted to the Vanderbilt Protein Mass Spectrometry Core Facility. Analysis of isolated GFP-tagged AKAP350A-scaffolded complexes by multidimensional protein identification technology (MudPIT) revealed two novel AKAP350A-interacting proteins. A summary of the MudPIT analysis is presented in Fig. 9*A*. The F2F3Δ1(1882–3907) fragment, but not shorter fragments, showed interactions with the $R_{II}\alpha$ subunit of protein kinase A, consistent with the mapping of protein kinase A anchoring sites in our previous investigations (13). We also identified both Cdk5RAP2 and Cep170 as proteins interacting specifically with AKAP350A truncation mutants containing the promoting region of AKAP350A (see Figs. 8 and 9*A*). These results suggest a role for AKAP350A as a coordinating center for regulation of

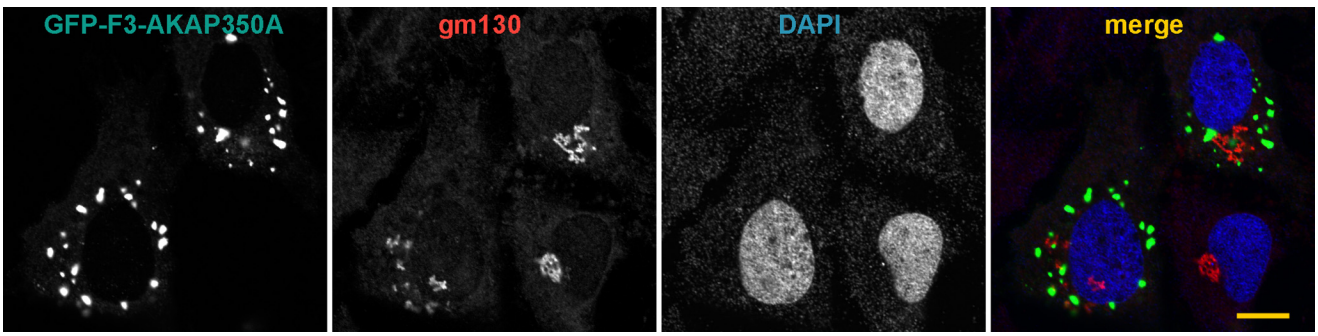

Figure 4. MTNCs induced by overexpression of EGFP-F3-AKAP350A are not Golgi-associated. HeLa cells transfected with EGFP-F3-AKAP350A were fixed with methanol and stained for the cis-Golgi marker gm130 (*red*) and DAPI (*blue*). Golgi cisternae were not associated with EGFP-F3-AKAP350A-expressing MTNCs. *Bar,* 10 μm.

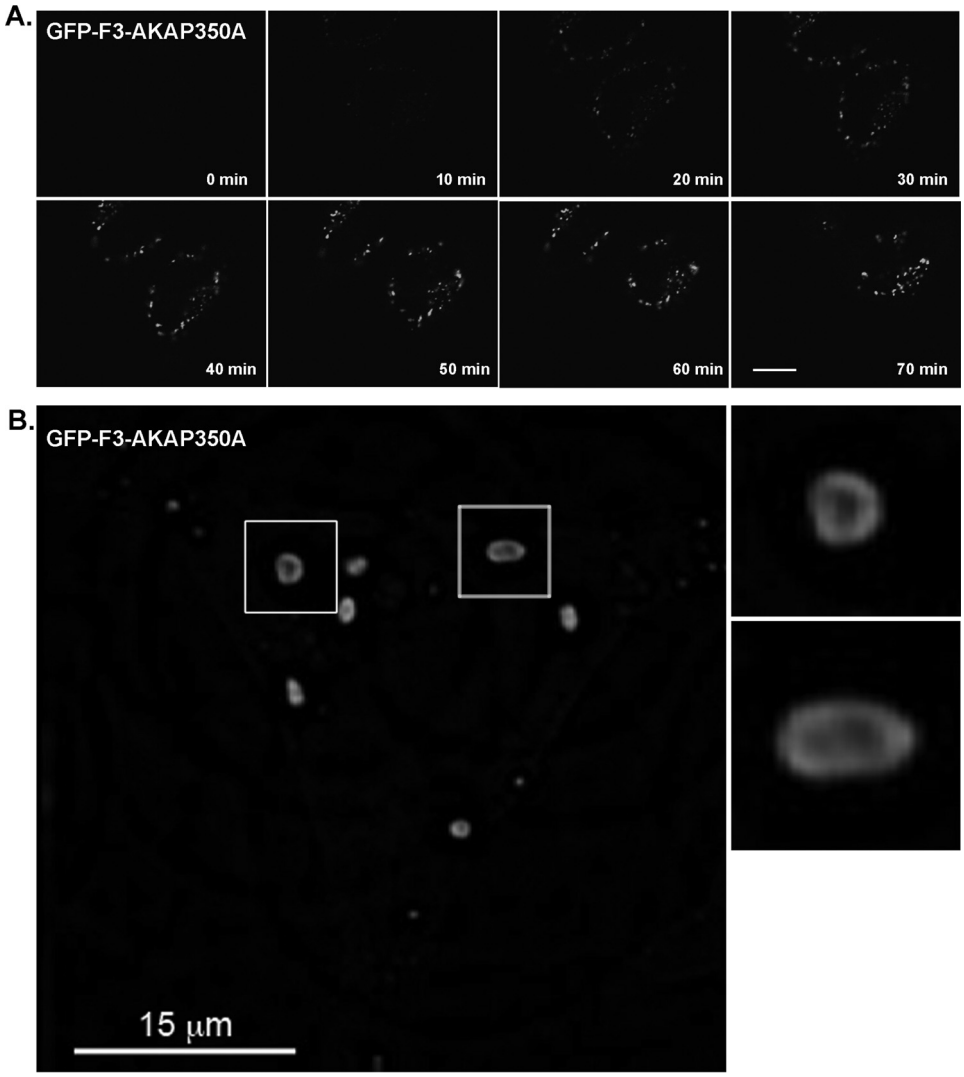

Figure 5. Visualization in live cells of MTNC formation induced by overexpression of EGFP-F3-AKAP350A. *A, de novo* formation of MTNCs induced by overexpression of EGFP-F3-AKAP350A. Video was initiated 6 h following transfection and recorded for 80 min. Snapshots from video were taken every 10 min using a Nikon A1R confocal microscope (see supplemental video S1). *B,* "donut-shaped" MTNCs induced by overexpression of EGFP-F3-AKAP350A. A snapshot from live imaging of GFP-F3-AKAP350A shows the presence of rings around MTNCs. The video was started 20 h after transfection and recorded for 2 h every 2 min using a DeltaVision deconvolution microscope (see supplemental Video S2). *Bar,* 15 μm.

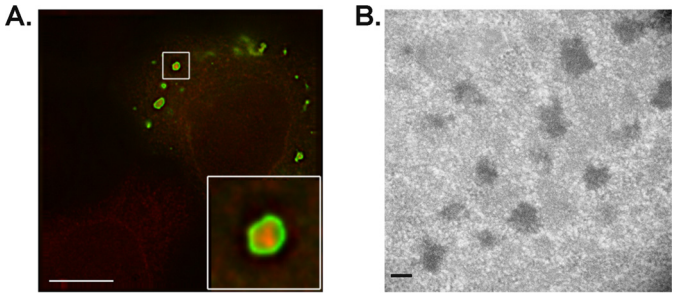

Figure 6. Structural assessment of MTNCs induced by overexpression of EGFP-F3-AKAP350A. *A,* DeltaVision deconvolution microscopy of MTNCs. Donut-shaped MTNCs induced by overexpression of EGFP-F3-AKAP350A include γ-tubulin (*red*) in the center hollow space. *Bar,* 15 μm. *B,* transmission electron microscopy of MTNCs. HeLa cells overexpressing EGFP-F3-AKAP350A were fixed, embedded, and processed for imaging with transmission electron microscopy. *Bar,* 100 nm.

microtubule nucleation through its interactions with both Cep170 and Cdk5RAP2 (29). Notably, we also found a novel association of Cep68 with AKAP350A, and this interaction was not dependent on the presence of the promoting region. Thus, Cep68 was found complexed with all tested AKAP350A truncations (Fig. 9*A*). These findings indicate that Cep68 interacts with the far C-terminal region of AKAP350A.

Validation of mass-spectrometry interaction findings

Interactions of AKAP350A with Cdk5RAP2, Cep170, and Cep68 were confirmed and mapped using immunoisolation of AKAP350A-scaffolded complexes followed by Western blotting (Fig. 10). To examine those interactions, we expressed in HEK cells EGFP-tagged AKAP350A constructs (full-length AKAP350A, F3Δ3-AKAP350A F3-AKAP350A, and F2F3Δ1-AKAP350A as described in Fig. 8) and EGFP as a control, and then we used GFP-binding protein-conjugated beads to isolate protein complexes (30). We used overexpressed Myc-tagged Cep68 protein to evaluate interactions with AKAP350A because we were not able to achieve a satisfactory level of detection of endogenous protein using available anti-Cep68 antibodies. As shown in Fig. 10, both Cdk5RAP2 and Cep170 were

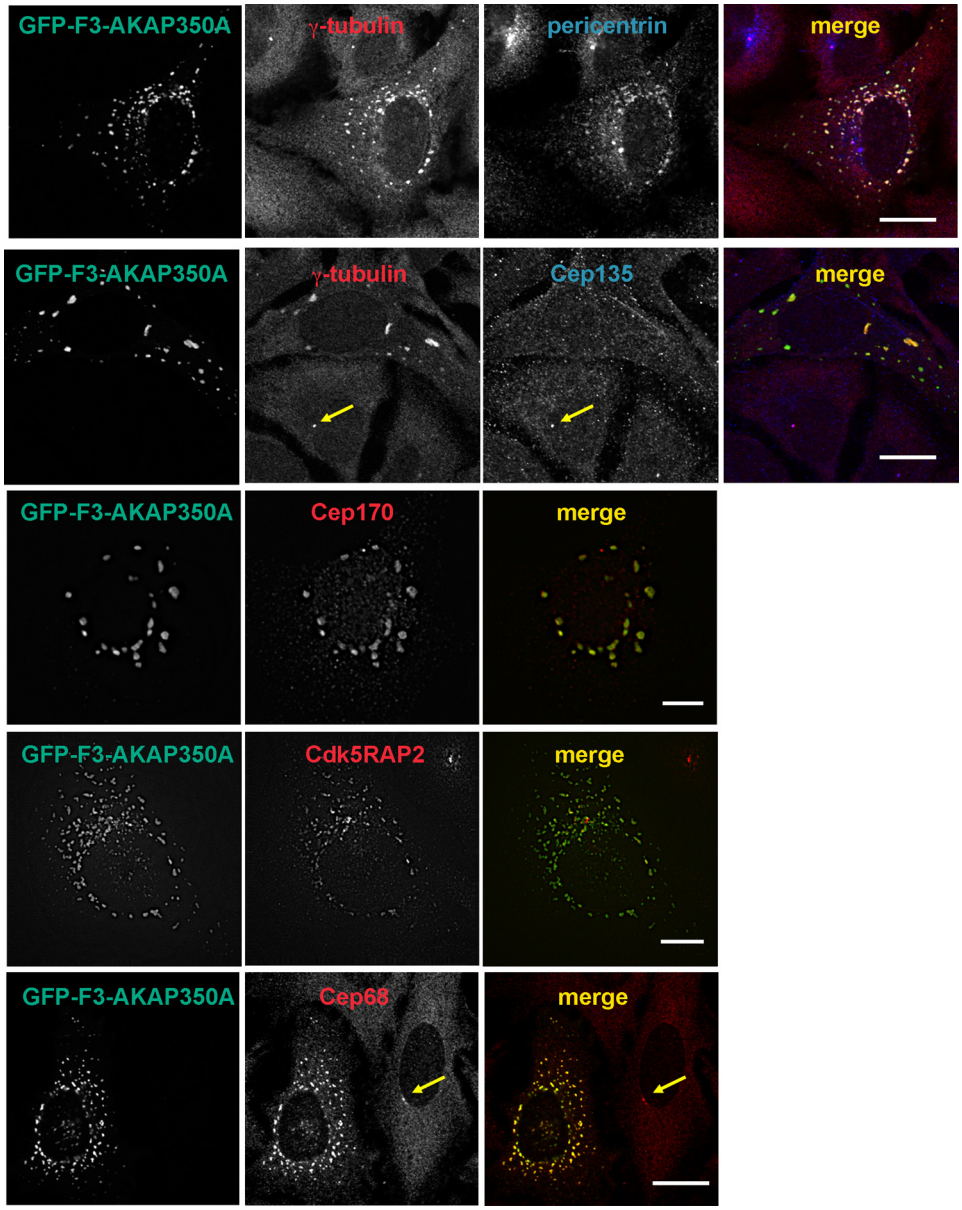

Figure 7. Endogenous γ-tubulin, pericentrin, Cep68, Cep170, and Cdk5RAP2 but not Cep135 co-localized with overexpressed of EGFP-F3-AKAP350A on MTNCs. HeLa cells were fixed with methanol or with 4% PFA for Cdk5RAP2 staining and immunostained for endogenous γ-tubulin (*red*), pericentrin. or Cep135 (*blue*), Cdk5RAP2, Cep170, Cep68 (*red*). (*Arrows* indicate non-transfected cells with a single centrosome.) The degree of co-localization between AKAP350A (*green*) and γ-tubulin/Cep170/Cdk5RAP2/Cep68 (*red*) or between AKAP350A (*green*) and pericentrin (*blue*) were quantified using PCC. PCCs were determined using JACOP plug-in of ImageJ software. PCC: γ-tubulin:AKAP350A 0.97 ± 0.06; pericentrin:AKAP350A 0.95 ± 0.11; Cep170:AKAP350A 0.96 ± 0.08; Cdk5RAP:AKAP350A 0.95 ± 0.09; Cep68:AKAP350A 0.98 ± 0.03). *Bar*, 15 μm.

specifically isolated only with AKAP350A mutants containing the promoting region (such as full-length AKAP350A, F3-AKAP350A, and F2F3Δ1-AKAP350A), but they were not observed in complex with F3Δ3-AKAP350A lacking the promoting region. In contrast, Cep68 was specifically isolated with all AKAP350A constructs. Therefore, the interaction between AKAP350A and Cep68 does not require the promoting region.

We next examined localization of mCherry-tagged chimeras for Cdk5RAP2, Cep170, and Cep68 co-expressed with EGFP-F3-AKAP350A in HeLa cells (supplemental Fig. S4). Overexpressed EGFP-F3-AKAP350A strongly overlapped with overexpressed mCherry-tagged Cep68, Cep170, and Cdk5RAP2 in supernumerary MTNCs.

Mapping of direct interactions within the AKAP350A–Cdk5RAP2–Cep170–Cep68 complex using yeast two-hybrid assays

We utilized binary yeast two-hybrid assays to elucidate whether the associations between various components of the AKAP350A–Cep170–Cdk5RAP2–Cep68 complex might be through direct interactions. Different parts of AKAP350A or full-length Cdk5RAP2 were cloned into a pBD-Gal bait vector, and full-length Cdk5RAP2, Cep170, and Cep68 were cloned into pAD target vectors (31). Binary assays were performed as shown on Fig. 9*B*. We were able to establish a direct interaction between AKAP350A and Cep170 and mapped that interaction

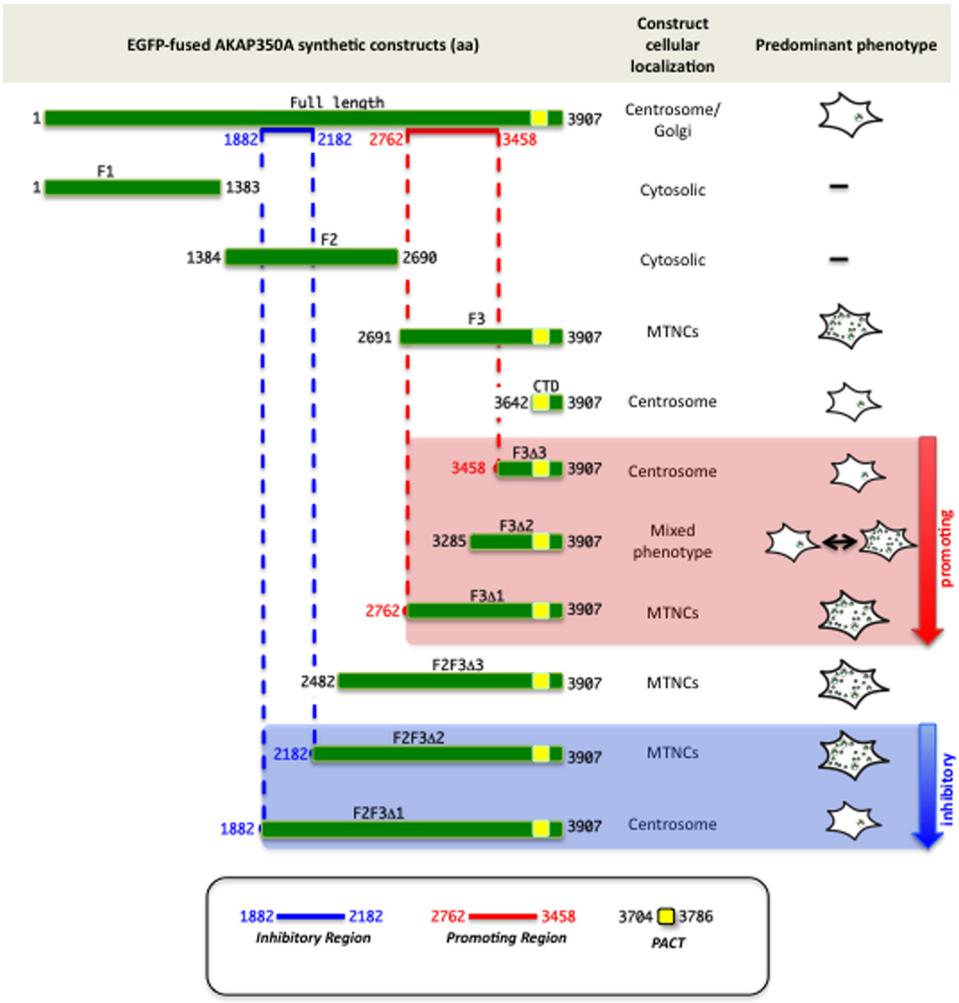

Figure 8. Mapping of AKAP350 regions responsible for the formation of supernumerary MTNCs. Schematic representation of full-length and truncations of synthetic EGFP-AKAP350A. Note the change of phenotype from single centrosome to multiple MTNCs with addition of promoting region (amino acids 2762–3458) and a change back to a single centrosome-targeted phenotype with the inhibitory region (amino acids 1882–2182). PACT, pericentrin-AKAP450 centrosomal targeting domain (amino acids 3704–3786). Quantification of predominant phenotype was performed for each EGFP-AKAP350A truncation using at least 100 cells overexpressing evaluated mutant; values are presented as percentage of cells with predominant phenotype (single centrosome or multiple MTNCs) from total number of cells expressing evaluated EGFP-AKAP350A. Data presented as average ± S.D. Full-length AKAP350 (centrosome 100 ± 0%), F2F3Δ1 (centrosome; 81 ± 9%), F2F3Δ2 (MTNCs; 82 ± 15%), F2F3Δ3 (MTNCs; 87 ± 7%), F3 (MTNCs; 92 ± 6%), F3Δ1 (MTNCs; 93 ± 4%), F3Δ2 (mixed phenotype; 54 ± 16% of MTNCs), F3Δ3 (centrosome; 93 ± 2%).

to the promoting region of AKAP350A(2762–3458) and the N-terminal region of Cep170(1–852) (Fig. 9*B*).

We were unable to detect any interaction between other components of the complex. Therefore, the interaction between AKAP350A and Cdk5RAP2–Cep68, as well as interactions between Cdk5RAP2–Cep170–Cep68 may be indirect or require multiple protein interactions, although we also recognize the possibility of false-negative results when using a two-hybrid system due to incompatibility of construct stoichiometry. Indeed, it should be noted, that AKAP450 was found in immunoprecipitates in complex with Cdk5RAP2(1726–1893) (29). Because of self-activation problems in yeast two-hybrid assays, the interaction between Cep68 and Cep170 was tested using a co-immunoprecipitation approach. EGFP-tagged Cep170 and Myc-tagged Cep68 were co-expressed in HEK cells; complexes were isolated using GFP-binding protein-conjugated magnetic beads, and complexes were analyzed for the presence of both GFP and Myc tags by Western blotting. Using this approach, we were not able to detect an interaction between Cep170 and Cep68 (data not shown).

Spatial relationship of AKAP350A with Cdk5RAP2–Cep170–Cep68

Although structural aspects of centriole assembly were revealed by cryo-electron microscopy (32–34), the spatial organization of various components remains incomplete. Recent studies utilizing super-resolution three-dimensional structured illumination microscopy (3D-SIM) have revealed a number of organizational features of the centrosome (9, 10). Nevertheless, the spatial organization of AKAP350A complexed with Cep170, Cep68, and Cdk5RAP2 remains unclear. We examined the locations of proteins of interest within the centrosome during interphase by both 3D-SIM super-resolution fluorescence microscopy (Fig. 11) and DeltaVision deconvolution microscopy (Fig. 12). Double labeling of endogenous AKAP350A and pericentrin resolved by super-resolution microscopy presented

A.

Number of peptides:			
AKAP9	**1104**	**1763**	**857**
RIIα	**2**	**2**	**42**
Cep170	**1**	**14**	**5**
Cdk5RAP2	**0**	**13**	**13**
Cep68	**9**	**6**	**3**

B.

pAD vectors	pBD vectors	
	Cdk5RAP2	**AKAP350A**
Cdk5RAP2	n/d	negative
Cep68	negative	negative
Cep170	negative	**positive**
Cep170(1-852)	n/d	**positive**

Figure 9. Analysis of proteins interacting with AKAP350A. *A,* spectral counts of peptides specifically isolated with GFP-chimeric AKAP350A truncation mutants. GFP-tagged truncation mutants of AKAP350A exhibiting different phenotypes were overexpressed in HEK cells, isolated with GFP-binding protein beads, and analyzed by MudPIT. *B,* yeast two-hybrid interactions. Yeast two-hybrid assays were performed with plasmids encoding the DNA-binding domain of GAL4 fused to AKAP350A or Cdk5RAP2 *versus* the activation domain of GAL4 fused to Cep68, Cep170, or Cdk5RAP2. Positive and negative colonies were identified as described under "Experimental procedures." Note that because of self-activation, the interaction between Cep68 and Cep170 was not tested using two-hybrid assays.

in Fig. 11 demonstrates that AKAP350A is located in the "bridge" connecting the two centriolar rings of pericentrin, as well as projecting from one centriole. Given that Cep68 as well as Cdk5RAP2 are implicated in centrosome cohesion, we also performed a triple labeling of AKAP350A–pericentrin–Cep68. Triple-color labeling resolved using DeltaVision deconvolution microscopy is presented in Fig. 12*A*. AKAP350A was distributed in juxtaposition with Cdk5RAP2, which generally co-distributed with pericentrin at both centrioles. AKAP350A was also observed in the bridge between centrioles. AKAP350A was additionally seen adjacent to the staining for Cep170 at the mother centriole. Finally, Cep68 appeared to distribute along AKAP350A staining, especially in the intercentriolar bridge region. Note that AKAP350A was situated alongside rootletin but also projected from one centriole (Fig. 12*B*). In view of these data, we propose that AKAP350A along with Cep68 serves as a component of the link connecting the two centrioles, providing a scaffolding support for Cep68 (see model in Fig. 13).

Loss of AKAP350A leads to Cep68 and Cep170 displacement from centrosome

To evaluate further the composition of protein complexes scaffolded by AKAP350A, we performed AKAP350A depletion by short interference RNA (siRNA) in both U2OS and HeLa cells. It should be noted that endogenous AKAP350A is commonly distributed between centrosomes and the Golgi apparatus in the majority of cells. The pattern for endogenous AKAP350A staining changes between different cell types, and it is noticeable that HeLa cells have a more pronounced Golgi-targeted pool of AKAP350A than in U2OS cells. Therefore, although effects of AKAP350A depletion on centrosome composition were similar in U2OS cells (Fig. 14) and HeLa cells (supplemental Fig. S5 and data not shown), the effect of AKAP350A depletion on centrosomal composition was more apparent in U2OS cells with less Golgi-targeted AKAP350A. Depletion AKAP350A caused displacement from the centrosomes of both Cep68 and Cep170 (Fig. 14). Also, although reduction of AKAP350A expression led to displacement of the Golgi-targeted pool of Cdk5RAP2, it did not affect the localization of the centrosome-targeted pool of Cdk5RAP2, in agreement with a previously published report (29). Reduction of AKAP350A expression did not affect the localization of γ-tubulin (supplemental Fig. S6). Cells with loss of AKAP350A at the centrosome were identified and coded for the presence or absence of co-stained centrosomal protein. Thirteen of 14 cells lacking AKAP350A were also negative for Cep68 at the centrosome. Similarly, 13 of 14 cells without AKAP350A expression also lacked Cep170 at the centrosome. In contrast, 12 of 12 cells lacking AKAP350A were still positive for Cdk5RAP2 at the centrosome, and 10 of 10 were positive for γ-tubulin. These findings suggest that AKAP350A is responsible for scaffolding Cap170 and Cep68 at the centrosome ($p = 0.004$ by Wilcoxon Signed Rank test).

Discussion

We have found evidence for scaffolding/recruitment by AKAP350A of multiple centrosomal proteins that are all associated with regulation of microtubule nucleation. Expression of

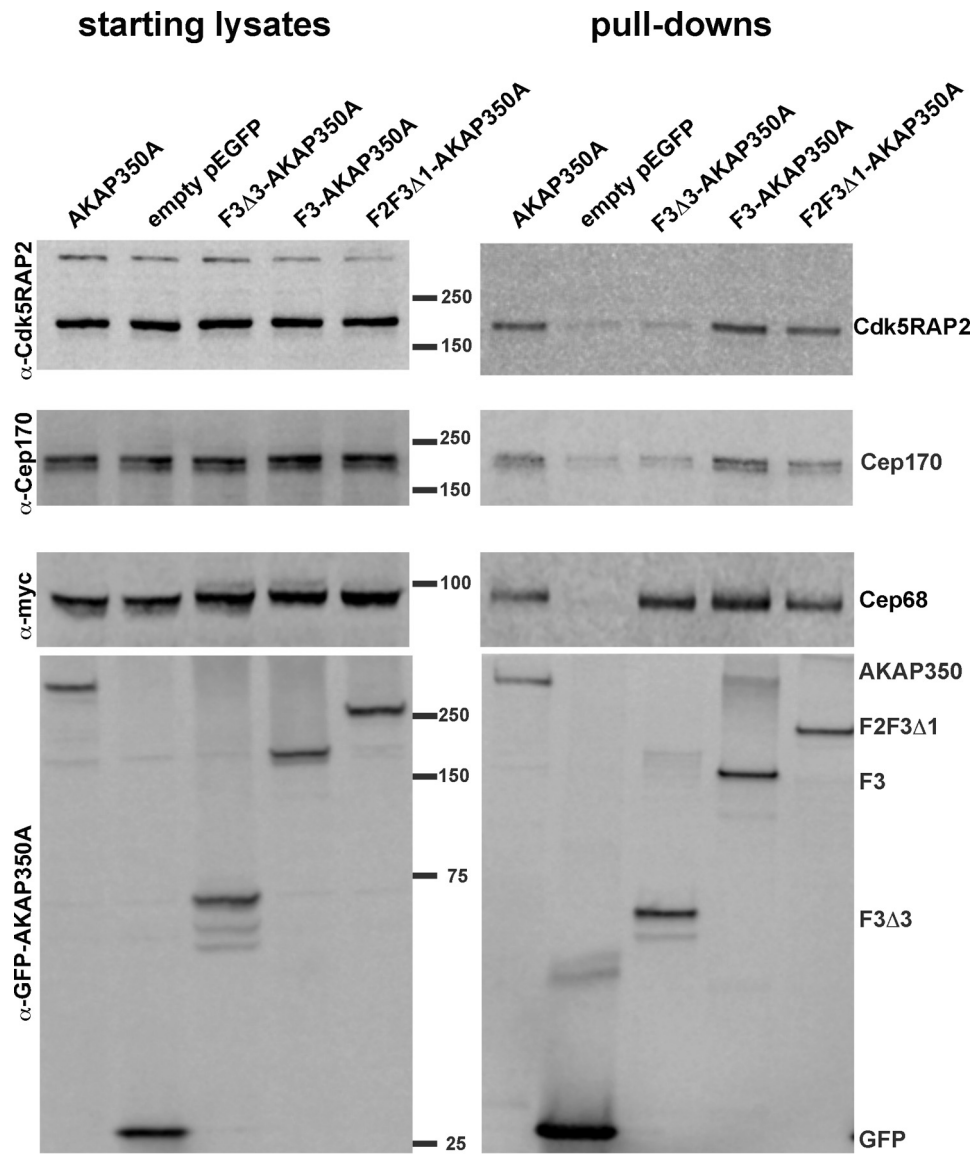

Figure 10. AKAP350A association with Cdk5RAP2, Cep170, and Cep68 proteins. EGFP-tagged AKAP350A constructs including full-length AKAP350A, empty pEGFP-C1, F3D3-AKAP350A, F3-AKAP350A, or F2F3D1-AKAP350A vectors were expressed in HEK-293T cells or co-expressed with Myc-tagged Cep68. Proteins isolated using GFP-binding protein conjugated beads were probed either for endogenous Cdk5RAP2 and Cep170 or for Myc tag (to detect Cep68) and for GFP (to detect AKAP350A). Empty pEGFP-C1 vector was used as a negative control. Dual detection was performed on the same membrane for both GFP and Cdk5RAP2/Cep170 or GFP and Myc tag using Odyssey LiCor system. Results are representative of three independent experiments.

a C-terminal truncation mutant of AKAP350A, encompassing the C-terminal third of the protein, induced formation of multiple γ-tubulin-containing units, which served as functional MTNCs. Live imaging of the formation of MTNCs demonstrated that the MTNCs developed *de novo*. Structural analysis of MTNCs by both high-resolution deconvolution microscopy and transmission electron microscopy revealed that EGFP-F3-AKAP350A-induced MTNCs consist of symmetrical structures as opposed to merely agglomerates of recruited proteins. Various centrosomal proteins such as γ-tubulin, pericentrin, Cdk5RAP2, Cep170, and Cep68, but not centriolar markers, were recruited to newly-formed MTNCs, suggesting that EGFP-F3-AKAP350A-induced MTNCs are not "complete centrosomes" but rather functional microtubule nucleation centers located in cytoplasm.

Interestingly, Fong *et al.* (35) reported that a cytoplasmic pool of overexpressed Cdk5RAP2 formed clusters of different sizes during disruption of microtubules with nocodazole treatment. Furthermore, these clusters formed microtubule asters upon nocodazole removal. These results are similar to the pattern of multiple MTNC formation caused by the overexpression of the C-terminal third of AKAP350A, which also can recruit Cdk5RAP2. Interestingly, Cdk5RAP2 loss of function in mice causes centrosome amplification and leads to multiple cilia formation (36).

A number of pericentriolar proteins, including percentrin (37), AKAP350 (22), and Cdk5RAP2 (35), serve as γ-tubulin ring complex (γ-TuRC) recruiters to centrosomes directly or indirectly as a part of pericentriolar matrix. Although some pericentriolar proteins such as AKAP350 and Cdk5RAP2 are

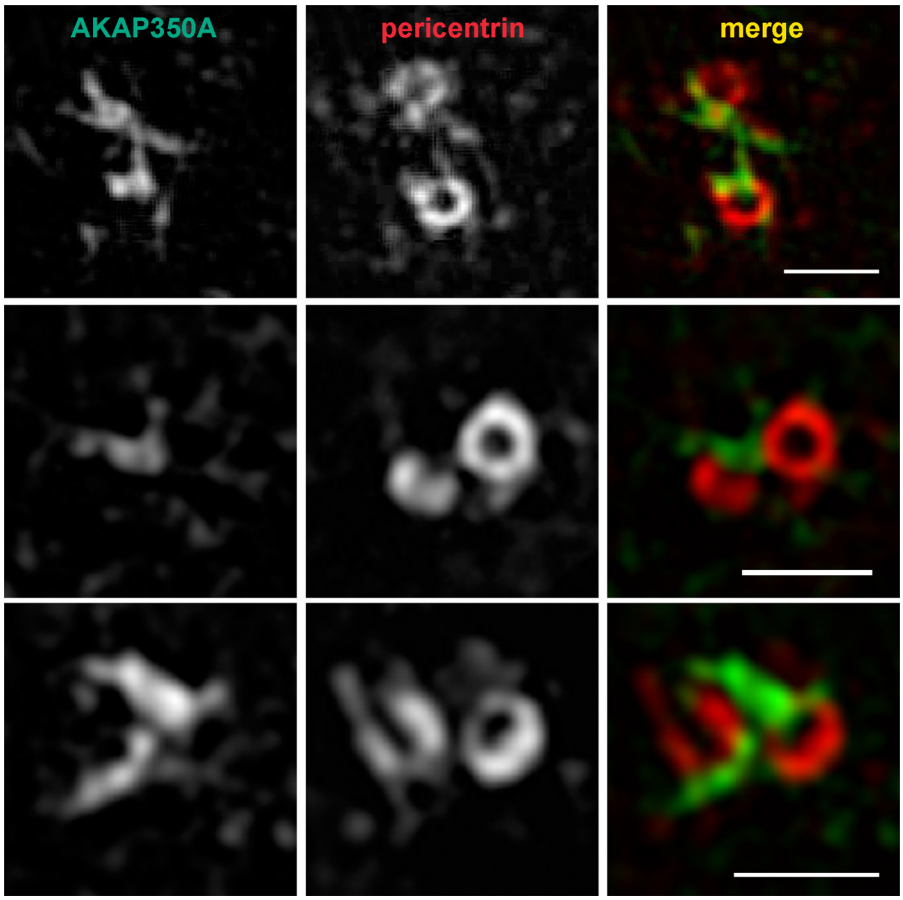

Figure 11. AKAP350A resides within linker connecting centrioles. HeLa cells were fixed with cold methanol and stained for endogenous AKAP350A (*green*) and pericentrin (*red*). Images were taken using 3D-SIM super-resolution fluorescence microscopy (OMX Blaze). Note the distribution of AKAP350A between the centrioles. *Bar,* 1 μm.

also part of microtubule nucleation complexes located at the Golgi apparatus, here we demonstrated that supernumerary MTNCs initiated by overexpression of EGFP-AKAP350A are Golgi-independent.

We identified the region between amino acids 2762 and 3458 of AKAP350A as a "promoting region," which is essential for multiple MTNC formations caused by EGFP-F3-AKAP350A overexpression. We also were able to identify a separate inhibitory region (amino acids 1882–2182) in AKAP350A upstream of the promoting region, which conferred a loss of supernumerary MTNC formation. This inhibitory region prevented supernumerary MTNC formation even in *trans* when both constructs were co-expressed. Thus, AKAP350A function may be regulated by the assembly of functional AKAP350A oligomer complexes or other intramolecular inhibitory interactions. AKAP350A appears to coordinate multiple signals that influence decisions involved in microtubule nucleation process at the centrosome.

We have found evidence for scaffolding by AKAP350A of multiple centrosomal proteins that are all associated with regulation of centrosome function. Mass spectrometry analysis of different AKAP350A-scaffolded protein complexes revealed that two centrosomal proteins, Cdk5RAP2 and Cep170, interact specifically with AKAP350A constructs containing the MTNC-promoting region and therefore likely play roles in regulation of microtubule nucleation. Another centrosomal protein, Cep68, associated with AKAP350A distal to the promoting region in the far C-terminal sequence of AKAP350A, which also contains the PACT domain and the binding region for TACC3 (31).

The results presented here support the concept that AKAP350A may coordinate the dynamic association of Cdk5RAP2 and Cep68 at the centrosome. Cyclin-dependent kinase 5 regulatory subunit-associated protein 2 (Cdk5RAP2/Cep215) localizes at centrosome during cell division and at the Golgi apparatus in interphase cells (38). Cdk5RAP2 function is required for astral microtubule formation during mitosis and for microtubule organization by the centrosome. Cdk5RAP2 also promotes microtubule nucleation by γTuRC (39), and depletion of Cdk5RAP2 by siRNA impairs γTuRC association with the centrosome (35). Phosphorylation of Cdk5RAP2 is crucial for CDK5RAP2-dependent microtubule nucleation and therefore correct spindle orientation (40). Structurally, an interaction of Cdk5RAP2 with pericentrin is essential for centrosome maturation and bipolar spindle formation during mitosis (41) and recruitment of Cdk5RAP2 to centrosomes is microtubule- and dynein-dependent (42). A previous investigation has noted that the centrosome-targeting domain of Cdk5RAP2 can interact with both pericentrin and AKAP350 (29). Cdk5RAP2 connects centrosomes to mitotic spindle poles marked by TACC3, which also can be scaffolded by AKAP350 (31, 43). Interestingly, Cdk5RAP2 is required for targeting of AKAP350 to spindle

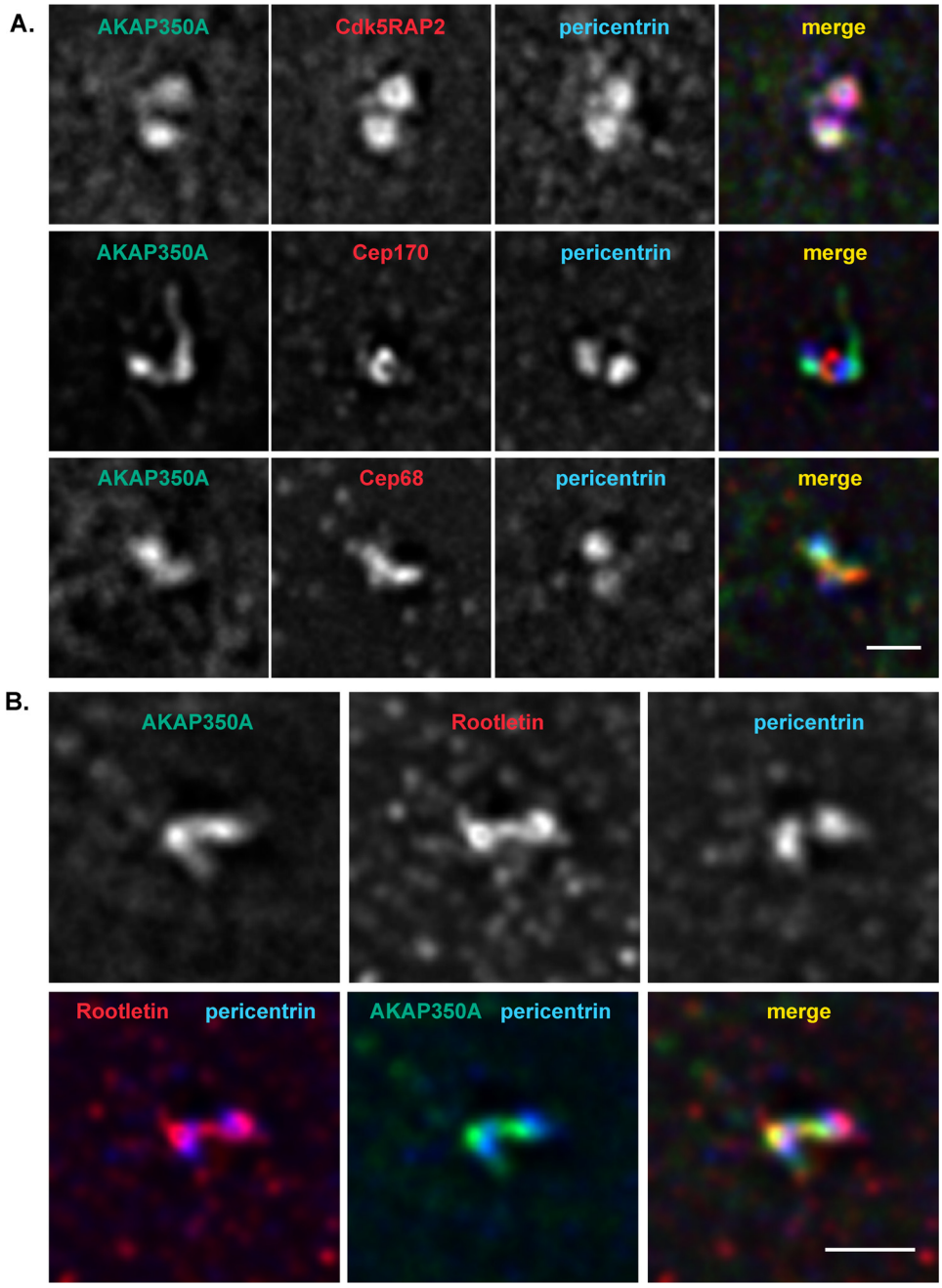

Figure 12. AKAP350A, together with Cep68, spans the linker connecting centrioles. *A,* HeLa cells were fixed with cold methanol or 4% PFA for Cdk5RAP2 staining and stained for AKAP350A (*green*) and Cdk5RAP2, Cep170, or Cep68 (*red*) and pericentrin (*blue*). Images were taken using DeltaVision deconvolution fluorescence microscopy. *Bar 1,* μm (applies to all images). *B,* HeLa cells were fixed with cold methanol and stained for AKAP350A (*green*), rootletin (*red*), and pericentrin (*blue*). Images were taken using DeltaVision deconvolution fluorescence microscopy. *Bar,* 1 μm (applies to all images).

poles during mitosis, but interphase centrosomal localization of AKAP350 seems to be Cdk5RAP2-independent (43). In support of this concept, loss of AKAP350 following siRNA depletion did not alter Cdk5RAP2 association with the centrosome. Both Cdk5RAP2 and Cep68 were identified as proteins involved in centrosome cohesion using an siRNA screening approach, as their depletion produced substantial centrosome splitting (45). Subcellular localization of Cep68 resembles the pattern for rootletin fibers connecting centrioles, whereas Cdk5RAP2 is associated with centriolar cylinders (45). Rootletin forms centriole-associated fibers and is implicated in centrosome cohesion (46). Cep68 is degraded in prometaphase, allowing centrosome separation, and Cep68 degradation is initiated by its phosphorylation on serine 332 by Plk1 (47). Different pools of Cdk5RAP2 bind to either Cep68 or pericentrin, and centriole disengagement is promoted by Cdk5RAP2 release from both pools, either by Cep68 degradation or by pericentrin cleavage (47).

Cep170 was identified by a two-hybrid screen as an interacting protein for Polo-like kinase 1 (Plk1) and is phosphorylated during mitosis (48). Cep170 associates with centrosomes during interphase and with spindle microtubules during mitosis (48). Interestingly, the sites phosphorylated *in vitro* by Plk1, the Plk1–Cep170 interaction domain, and the centrosomal target-

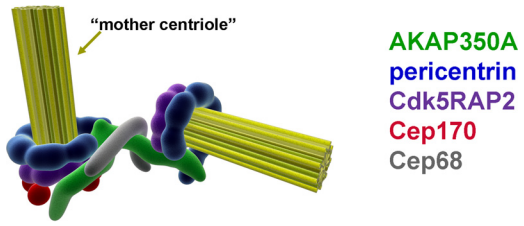

Figure 13. Schematic representation of the assembly of proteins in the centrioles and the bridge connecting two centrioles. Both pericentrin and Cdk5RAP2 form ring-like structures around the bases of both centrioles. In contrast, Cep170 is only associated with mother centriole. AKAP350A is observed in the bridge between centrioles as well as adjacent to the staining for Cep170 at the mother centriole. Cep68 appeared to distribute along AKAP350A staining in the intercentriolar bridge region.

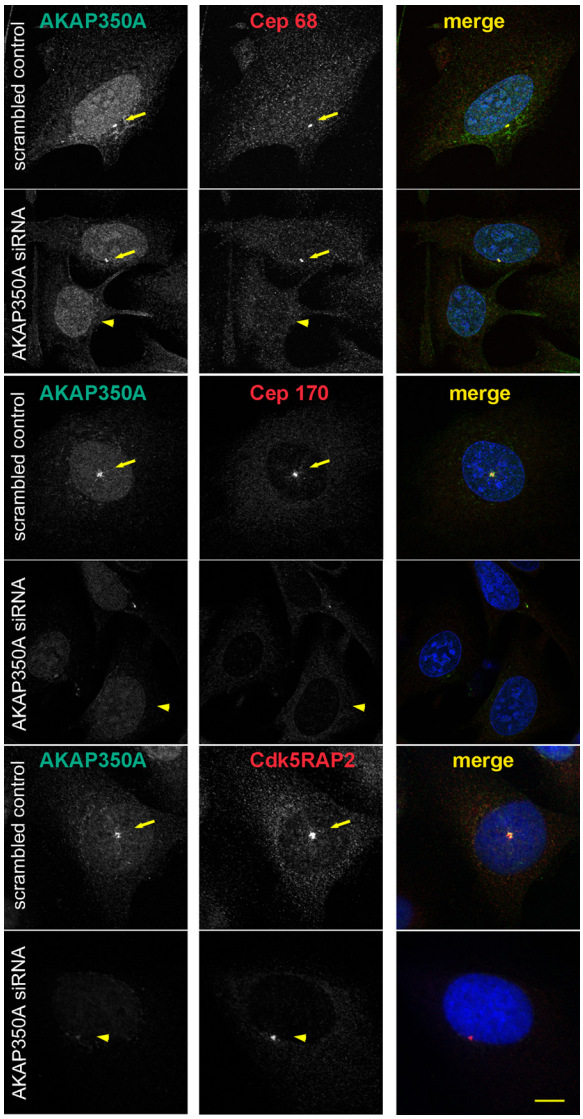

Figure 14. Depletion of AKAP350A by siRNA interference. U2OS cells were transfected with either non-specific scrambled RNA duplexes or siRNA duplexes specific for AKAP350A, fixed, and dual-stained for AKAP350A (*green* in merged images) and Cep68, Cep170, or Cdk5RAP2 (*red* in merged images). *Arrows* indicate cells with AKAP350A at centrosomes. *Arrowheads* indicate cells with loss of AKAP350A. Depletion of AKAP350A caused loss of both Cep68 and Cep170 from the centrosome, but Cdk5RAP2 localization at the centrosome was not affected. *Bar,* 10 μm (applies to all images).

ing domain of Cep170 all map to the C-terminal half of the protein (48), whereas we mapped the AKAP350A interaction to an N-terminal region of Cep170 (amino acids 1–852). Both overexpression and depletion experiments suggested a role for Cep170 in microtubule organization (48). Cep170 is associated with subdistal appendages typical of the mother centriole and therefore serves as a marker of centriole maturation (48).

Using super-resolution microscopy, we determined that endogenous AKAP350A is located within the intercentriolar linker in conjunction with Cep68. Cep68 together with Cdk5RAP5 were shown previously to play roles in centrosome cohesion and engagement in interphase (45, 47, 49). Plk1 phosphorylation of Cep68 at Ser-322 initiates the degradation of Cep68 during prometaphase, allowing Cdk5RAP2 removal and centriole disengagement (47). Cep68 is also phosphorylated by Nek2A both *in vitro* and *in vivo* (13, 28, 50), and this phosphorylation also promotes Cep68 degradation in mitosis. Our SIM studies also supported the presence of Cep170 at the mother centriole and Cdk5RAPs at the bases of both centrioles, in both cases juxtaposed to AKAP350 in the intercentriolar bridge. Interestingly, the expressed C-terminal construct of AKAP350A that can interact with both Cep170 and Cdk5RAP2 was distributed in rings, a morphology quite different from that observed at the centrosomes. These data suggest that the N-terminal regions of AKAP350A may be associated with the intercentriolar bridge, although we should note that expression of a construct containing the N-terminal two-thirds of AKAP350A failed to target to the centrosomes. Considering that the expression of the carboxyl third of AKAP350A induced the formation of multiple functional MTNCs, it appears likely that AKAP350A connections through the intercentriolar bridge are involved in regulating the microtubule nucleation process at the centrosome. Depletion of AKAP350A by siRNA displaced Cep68 and Cep170, but not Cdk5RAP2 from the centrosome, suggestive of a role for AKAP350A as an organizing scaffold for various regulatory proteins at the centrosome.

In summary, we have analyzed truncation mutants of AKAP350A for their ability to induce the formation of supernumerary MTNCs and identified functional regions regulating microtubule nucleation at cytoplasmic Golgi-independent microtubule nucleation centers. Although the role of AKAP350A in microtubule nucleation is recognized at both centrosome and Golgi apparatus, here we have presented the first evidence that overexpression of the C-terminal third of AKAP350A is sufficient for recruitment of various pericentriolar proteins and "*de novo*" formation of cytoplasmic MTNCs. Finally, we have identified two previously unrecognized AKAP350A-interacting proteins, Cep170 and Cep68, and mapped a direct interaction between the promoting region of AKAP350A(2762–3458) and the N-terminal region of Cep170(1–852). Super-resolution microscopy has allowed construction of a model of centriole structure that now includes the participation of AKAP350A in the intercentriolar linker as well as at the centrioles (Fig. 13). The association of AKAP350A with Cdk5RAP2, Cep170, and Cep68 suggests that complexes of these proteins may regulate proteins associating with the intercentriolar bridge and their contribution to microtubule nucleation at the centrosome.

Experimental procedures

Cell culture

HeLa cells (American Type Culture Collection, ATCC) were maintained at 37 °C in 5% CO_2 using complete RPMI 1640 media supplemented with 10% fetal bovine serum (FBS). HEK-293 and U2OS cells (ATCC) were maintained at 37 °C in 5% CO_2 using complete DMEM supplemented with 10% fetal bovine serum (FBS). Cells were transfected using PolyJet (SignaGen) according to the manufacturer's protocol.

GFP-AKAP350A assembly

Synthetic constructs of AKAP350A fragments were synthesized by GeneART (Thermo Fisher Scientific). Amino acids 1–1400 were received as fragment 1 (F1) in a modified pEGFP vector missing the HindIII site normally in the multicloning site. Amino acids 1360–2700 were received as fragment 2 (F2) in pMA vector. Finally, amino acids 2689–3907 were received as fragment 3 (F3) in a pMA vector. AKAP350A-F3 was subcloned into pEFGP-C3 using the XhoI and BamHI restriction site. Assembly of full-length AKAP350A was achieved via triple ligation at 16 °C overnight using pEGFP-AKAP350A-F1 (cut with HindII and BamHI), AKAP350A-F2 (cut from pMA with HindIII and XhoI), and AKAP350A-F3 (cut with XhoI and BamHI). Truncation mutants of AKAP350A used in mapping of functional regions of AKAP350A were cloned using primers summarized in supplemental Table S1.

Plasmid construction

Human Cep170 and Cdk5RAP2 were amplified from cDNA clones available from Transomic (Huntsville, AL); human Cep68 was amplified from human liver cDNA as summarized in supplemental Table S1. pmCherry-C1 and pmCherry-C2 vectors were gifts from Dr. Roger Tsien, University of California, San Diego.

Fluorescence microscopy and analysis

HeLa cells grown on collagen-coated coverslips were fixed either with methanol for 5 min at −20 °C or at room temperature for 15 min using 4% paraformaldehyde (PFA) supplemented with 0.1% Triton X-100, 80 mM potassium/PIPES, pH 7.2, 1 mM EGTA, 1 mM $MgSO_4$, and 30% glycerol, followed by permeabilization with 0.25% Triton X-100. Fixed cells were blocked with 5% normal serum for 1 h at room temperature and then were incubated with primary antibodies for 1 h at room temperature: rabbit anti-Cep170 (1:100; Sigma); rabbit anti-Cep68 (1:100; Sigma); rabbit anti-Cdk5RAP2 (1:100; Sigma); mouse anti-AKAP350, 14G2 clone (1:200), mouse anti-gm130 (1:300; BD Biosciences); rabbit anti-pericentrin (1:700; Sigma); rabbit anti-γ-tubulin (1:700; Sigma); rabbit anti-rootletin (1:200; Sigma). This was followed by incubation at room temperature for 1 h with species-specific fluorescent secondary antibodies conjugated with Alexa-488, Alexa-568, or Alexa-647 (1:500; Life Technologies, Inc.). Coverslips were mounted using Prolong Gold with DAPI (Invitrogen). Confocal fluorescence microscopy was performed using a ×60 or ×100 oil immersion lens on an Olympus FV-1000 confocal fluorescence microscope (Vanderbilt Cell Imaging Shared Resource). Live-cell imaging was performed using a DeltaVision deconvolution live cell microscope or a Nikon A1-R confocal microscope (Digital Histology Shared Resource, Vanderbilt University). For imaging centrosome architecture, 3D-SIM super-resolution fluorescence microscopy was applied (OMX Blaze, Vanderbilt Cell Imaging Shared Resource).

Cell quantitative analysis and statistical analysis

All experiments were performed at least three times. Quantification of centrosome phenotype (single centrosome *versus* multiple MTNCs, Fig. 8) was performed using at least 100 cells overexpressing each EGFP-AKAP350 mutant. The percentage of cells demonstrating a particular phenotype was calculated in each ×20 magnification field; at least five fields were analyzed for each mutant.

The degree of co-localization between AKAP350A and γ-tubulin–Cep170–Cdk5RAP2–Cep68–pericentrin was quantified using Pearson's correlation coefficient (PCC). Cells overexpressing either EGFP-F3-AKAP350A (when stained for endogenous interacting proteins) or both EGFP-F3-AKAP350A and Cherry-tagged Cep68–Cep170–Cdk5RAP2 were outlined with the ImageJ free-selection tool, and PCC was calculated for overexpressing cells only. PCCs were determined using JACOP plug-in of ImageJ software. At least 10 cells were analyzed for each evaluated protein.

The sizes of microtubule "asters" originating from either centrosome MTOCs or ectopic MTNCs during recovery following nocodazole treatment were determined using ImageJ software (National Institutes of Health) for at least 10 cells overexpressing EGFP-F3-AKAP350A *versus* at least 50 cells without AKAP350 overexpression. Changes in size were analyzed using a two-tailed *t* test with Welch's correction.

Statistics are detailed in the figure legends. All data are presented as average ± S.D.

Transmission electron microscopy

HeLa cells overexpressing EGFP-F3-AKAP350A were fixed, embedded, and processed for imaging with transmission electron microscopy. Specimens were processed for TEM and imaged in the Vanderbilt Cell Imaging Shared Resource–Research Electron Microscopy facility.

Embedding

Samples were fixed in 2.5% glutaraldehyde in 0.1 M cacodylate buffer, pH 7.4, at room temperature for 1 h and then transferred to 4 °C overnight. The samples were washed in 0.1 M cacodylate buffer, then incubated for 1 h in 1% osmium tetroxide at room temperature, and then washed with 0.1 M cacodylate buffer. Subsequently, the samples were dehydrated through a graded ethanol series and then three exchanges of 100% ethanol. Next, the samples were incubated for 5 min in 100% ethanol and propylene oxide (PO) followed by two exchanges of pure PO. Samples were then infiltrated with 25% Epon 812 resin and 75% PO for 30 min at room temperature. Next, they were infiltrated with Epon 812 resin and PO (1:1) for 1 h at room temperature and then overnight at room temperature. The next day, the samples went through a (3:1) (resin/PO) exchange for 3–4 h and then incubated with pure epoxy resin overnight.

Samples were then incubated in two more changes of pure epoxy resin and then allowed to polymerize at 60 °C for 48 h.

Sectioning and imaging

70–80-nm ultra-thin sections were cut and collected on 300-mesh copper grids and post-stained with 2% uranyl acetate and then with Reynold's lead citrate. Samples were subsequently imaged on the Philips/FEI Tecnai T12 electron microscope at various magnifications.

GFP pulldown and Western blotting

HEK-293T cells were either transfected with various GFP-tagged AKAP350A or empty pEGFP-C1 vectors alone (to evaluate interaction with endogenous Cdk5RAP2 and Cep170) or co-transfected with Myc-tagged Cep68 (to evaluate interaction with overexpressed Cep68). Cells were lysed 24 h after transfection using M-PER buffer (Pierce), supplemented with protease inhibitors and phosphatase inhibitors, for 15 min at room temperature, and then lysates were centrifuged at 16,000 × *g* for 10 min. Clarified lysates were incubated with GFP-binding protein-conjugated magnetic beads for 3 h at 4 °C. Beads were washed three times with TBS buffer and further analyzed by Western blotting using an Odyssey imager (LiCor). For detection of Cdk5RAP2 or Cep170, the same membrane was probed with either anti-Cdk5RAP2 (1:1000; Sigma) or Cep170 (1:1000; Sigma) rabbit polyclonal antibody simultaneously with anti-GFP monoclonal mouse antibody (Living Colors, Clontech). For detection of Cep68 immunoisolated by GFP-AKAP350A pulldowns, the same membrane was probed for both the GFP tag and Myc tag simultaneously with the primary antibodies 9E10-C2 mouse anti-Myc (1:1000; Vanderbilt Molecular Recognition Shared Resource) and rabbit anti-GFP (1:10,000; Abcam). This was followed by incubation with the IRDye secondary antibodies: donkey anti-mouse IRDye680RD (1:20,000) and donkey anti-rabbit IRDye800CW (1:20,000) (LiCor). 5% of sample was loaded as a starting material. Signal was detected using a LiCor Odyssey imager. Results are representative of three independent experiments.

Protein mass spectrometry

For mass spectrometry analysis, the eluted proteins were run into an 8% SDS-polyacrylamide gel; the gel was stained with GelCode Blue colloidal Coomassie Blue staining reagent (Pierce), and the stacked protein band at the interface of the stacking and resolving gel was excised and submitted for tryptic digest and analysis on LTQ linear ion trap mass spectrometer (Thermo Fisher Scientific, Vanderbilt Protein Mass Spectrometry Shared Resource).

Yeast two-hybrid assays

Yeast two-hybrid binary assays were performed as described previously (44). Briefly, full-length or truncation mutants of Cep170, Cdk5RAP2, and Cep68 were cloned into pAD-GAL4 and tested for interaction with various AKAP350A mutants in pBD-GAL4-Cam vector. Positive results were recorded if β-galactosidase assay was positive within 3 h. All constructs were tested for auto-activation. We used an established AKAP350-interacting protein, TACC3, cloned into pAD vector as a positive control for direct interaction (31). Results are representative of three independent experiments.

Depletion of AKAP350A

siRNA for AKAP350A knockdown was prepared as described previously (20). U2OS or HeLa cells were transfected with 30 nM siRNA duplexes using HiPerFect transfection reagent (Qiagen) and examined 48–72 h after transfection.

To analyze the effects of AKAP350A knockdown on the presence of other proteins at the centrosome, U2OS cells were stained for AKAP350A along with antibodies against Cep68, Cep170, Cdk5RAP2, or γ-tubulin. Cells with loss of AKAP350A at the centrosome were identified and coded for the presence or absence of co-stained centrosomal protein. The distribution of presence *versus* absence was analyzed by a Wilcoxon Signed Rank Test. At least 10 cells were analyzed for the presence of each protein.

Author contributions—E. K. designed and performed experiments, analyzed data, drafted and revised manuscript. J. T. R. designed and performed experiments and revised manuscript. L. A. L. designed and performed experiments, analyzed data, and revised manuscript. J. A. W. designed and performed experiments, analyzed data, and revised manuscript. T. A. M. designed and performed experiments, analyzed data, and revised manuscript. J. R. G. designed and performed experiments, analyzed data, and revised manuscript.

Acknowledgments—Fluorescence microscopy was performed through the use of the Vanderbilt University Cell Imaging Shared Resource, and MudPIT Proteomics was performed in the Vanderbilt Protein Mass Spectrometry Shared Resource supported by National Institutes of Health Grants S10 OD012324, CA68485, DK20593, DK58404, and HD15052. Deconvolution microscopy was performed in the Vanderbilt Digital Histology Shared Resource.

References

1. Alvey, P. L. (1985) An investigation of the centriole cycle using 3T3 and CHO cells. *J. Cell Sci.* **78,** 147–162
2. Kuriyama, R., and Borisy, G. G. (1981) Centriole cycle in Chinese hamster ovary cells as determined by whole-mount electron microscopy. *J. Cell Biol.* **91,** 814–821
3. Vorobjev, I. A., and Chentsov, YuS. (1982) Centrioles in the cell cycle. I. Epithelial cells. *J. Cell Biol.* **93,** 938–949
4. Bornens, M. (2012) The centrosome in cells and organisms. *Science* **335,** 422–426
5. Nigg, E. A., and Stearns, T. (2011) The centrosome cycle: centriole biogenesis, duplication and inherent asymmetries. *Nat. Cell Biol.* **13,** 1154–1160
6. Piel, M., Meyer, P., Khodjakov, A., Rieder, C. L., and Bornens, M. (2000) The respective contributions of the mother and daughter centrioles to centrosome activity and behavior in vertebrate cells. *J. Cell Biol.* **149,** 317–330
7. Andersen, J. S., Wilkinson, C. J., Mayor, T., Mortensen, P., Nigg, E. A., and Mann, M. (2003) Proteomic characterization of the human centrosome by protein correlation profiling. *Nature* **426,** 570–574
8. Jakobsen, L., Vanselow, K., Skogs, M., Toyoda, Y., Lundberg, E., Poser, I., Falkenby, L. G., Bennetzen, M., Westendorf, J., Nigg, E. A., Uhlen, M., Hyman, A. A., and Andersen, J. S. (2011) Novel asymmetrically localizing components of human centrosomes identified by complementary proteomics methods. *EMBO J.* **30,** 1520–1535
9. Lawo, S., Hasegan, M., Gupta, G. D., and Pelletier, L. (2012) Subdiffraction imaging of centrosomes reveals higher-order organizational features of pericentriolar material. *Nat. Cell Biol.* **14,** 1148–1158

10. Sonnen, K. F., Schermelleh, L., Leonhardt, H., and Nigg, E. A. (2012) 3D-structured illumination microscopy provides novel insight into architecture of human centrosomes. *Biol. Open* **1,** 965–976
11. Theurkauf, W. E., and Vallee, R. B. (1982) Molecular characterization of the cAMP-dependent protein kinase bound to microtubule-associated protein 2. *J. Biol. Chem.* **257,** 3284–3290
12. Lohmann, S. M., DeCamilli, P., Einig, I., and Walter, U. (1984) High-affinity binding of the regulatory subunit (RII) of cAMP-dependent protein kinase to microtubule-associated and other cellular proteins. *Proc. Natl. Acad. Sci. U.S.A.* **81,** 6723–6727
13. Schmidt, P. H., Dransfield, D. T., Claudio, J. O., Hawley, R. G., Trotter, K. W., Milgram, S. L., and Goldenring, J. R. (1999) AKAP350, a multiply spliced protein kinase A-anchoring protein associated with centrosomes. *J. Biol. Chem.* **274,** 3055–3066
14. Takahashi, M., Shibata, H., Shimakawa, M., Miyamoto, M., Mukai, H., and Ono, Y. (1999) Characterization of a novel giant scaffolding protein, CG-NAP, that anchors multiple signaling enzymes to centrosome and the Golgi apparatus. *J. Biol. Chem.* **274,** 17267–17274
15. Witczak, O., Skålhegg, B. S., Keryer, G., Bornens, M., Taskén, K., Jahnsen, T., and Orstavik, S. (1999) Cloning and characterization of a cDNA encoding an A-kinase anchoring protein located in the centrosome, AKAP450. *EMBO J.* **18,** 1858–1868
16. Kolobova, E., Efimov, A., Kaverina, I., Rishi, A. K., Schrader, J. W., Ham, A. J., Larocca, M. C., and Goldenring, J. R. (2009) Microtubule-dependent association of AKAP350A and CCAR1 with RNA stress granules. *Exp. Cell Res.* **315,** 542–555
17. Mason, T. A., Kolobova, E., Liu, J., Roland, J. T., Chiang, C., and Goldenring, J. R. (2011) Darinaparsin is a multivalent chemotherapeutic which induces incomplete stress response with disruption of microtubules and Shh signaling. *PLoS ONE* **6,** e27699
18. Rivero, S., Cardenas, J., Bornens, M., and Rios, R. M. (2009) Microtubule nucleation at the cis-side of the Golgi apparatus requires AKAP450 and GM130. *EMBO J.* **28,** 1016–1028
19. Wu, J., de Heus, C., Liu, Q., Bouchet, B. P., Noordstra, I., Jiang, K., Hua, S., Martin, M., Yang, C., Grigoriev, I., Katrukha, E. A., Altelaar, A. F., Hoogenraad, C. C., Qi, R. Z., Klumperman, J., and Akhmanova, A. (2016) Molecular pathway of microtubule organization at the Golgi apparatus. *Dev. Cell* **39,** 44–60
20. Larocca, M. C., Jin, M., and Goldenring, J. R. (2006) AKAP350 modulates microtubule dynamics. *Eur. J. Cell Biol.* **85,** 611–619
21. Tonucci, F. M., Hidalgo, F., Ferretti, A., Almada, E., Favre, C., Goldenring, J. R., Kaverina, I., Kierbel, A., and Larocca, M. C. (2015) Centrosomal AKAP350 and CIP4 act in concert to define the polarized localization of the centrosome and Golgi in migratory cells. *J. Cell Sci.* **128,** 3277–3289
22. Takahashi, M., Yamagiwa, A., Nishimura, T., Mukai, H., and Ono, Y. (2002) Centrosomal proteins CG-NAP and kendrin provide microtubule nucleation sites by anchoring γ-tubulin ring complex. *Mol. Biol. Cell* **13,** 3235–3245
23. Keryer, G., Witczak, O., Delouvée, A., Kemmner, W. A., Rouillard, D., Tasken, K., and Bornens, M. (2003) Dissociating the centrosomal matrix protein AKAP450 from centrioles impairs centriole duplication and cell cycle progression. *Mol. Biol. Cell* **14,** 2436–2446
24. Mattaloni, S. M., Ferretti, A. C., Tonucci, F. M., Favre, C., Goldenring, J. R., and Larocca, M. C. (2013) Centrosomal AKAP350 modulates the G/S transition. *Cell. Logist.* **3,** e26331
25. Gillingham, A. K., and Munro, S. (2000) The PACT domain, a conserved centrosomal targeting motif in the coiled-coil proteins AKAP450 and pericentrin. *EMBO Rep.* **1,** 524–529
26. Shanks, R. A., Steadman, B. T., Schmidt, P. H., and Goldenring, J. R. (2002) AKAP350 at the Golgi apparatus. I. Identification of a distinct Golgi apparatus targeting motif in AKAP350. *J. Biol. Chem.* **277,** 40967–40972
27. Baetz, N. W., and Goldenring, J. R. (2013) Rab11-family interacting proteins define spatially and temporally distinct regions within the dynamic Rab11a-dependent recycling system. *Mol. Biol. Cell* **24,** 643–658
28. Man, X., Megraw, T. L., and Lim, Y. P. (2015) Cep68 can be regulated by Nek2 and SCF complex. *Eur. J. Cell Biol.* **94,** 162–172
29. Wang, Z., Wu, T., Shi, L., Zhang, L., Zheng, W., Qu, J. Y., Niu, R., and Qi, R. Z. (2010) Conserved motif of CDK5RAP2 mediates its localization to centrosomes and the Golgi complex. *J. Biol. Chem.* **285,** 22658–22665
30. Rothbauer, U., Zolghadr, K., Muyldermans, S., Schepers, A., Cardoso, M. C., and Leonhardt, H. (2008) A versatile nanotrap for biochemical and functional studies with fluorescent fusion proteins. *Mol. Cell. Proteomics* **7,** 282–289
31. Steadman, B. T., Schmidt, P. H., Shanks, R. A., Lapierre, L. A., and Goldenring, J. R. (2002) Transforming acidic coiled-coil-containing protein 4 interacts with centrosomal AKAP350 and the mitotic spindle apparatus. *J. Biol. Chem.* **277,** 30165–30176
32. Guichard, P., Chrétien, D., Marco, S., and Tassin, A. M. (2010) Procentriole assembly revealed by cryo-electron tomography. *EMBO J.* **29,** 1565–1572
33. Li, S., Fernandez, J. J., Marshall, W. F., and Agard, D. A. (2012) Three-dimensional structure of basal body triplet revealed by electron cryo-tomography. *EMBO J.* **31,** 552–562
34. Jana, S. C., Marteil, G., and Bettencourt-Dias, M. (2014) Mapping molecules to structure: unveiling secrets of centriole and cilia assembly with near-atomic resolution. *Curr. Opin. Cell Biol.* **26,** 96–106
35. Fong, K. W., Choi, Y. K., Rattner, J. B., and Qi, R. Z. (2008) CDK5RAP2 is a pericentriolar protein that functions in centrosomal attachment of the γ-tubulin ring complex. *Mol. Biol. Cell* **19,** 115–125
36. Barrera, J. A., Kao, L. R., Hammer, R. E., Seemann, J., Fuchs, J. L., and Megraw, T. L. (2010) CDK5RAP2 regulates centriole engagement and cohesion in mice. *Dev. Cell* **18,** 913–926
37. Zimmerman, S., and Chang, F. (2005) Effects of γ-tubulin complex proteins on microtubule nucleation and catastrophe in fission yeast. *Mol. Biol. Cell* **16,** 2719–2733
38. Kraemer, N., Issa, L., Hauck, S. C., Mani, S., Ninnemann, O., and Kaindl, A. M. (2011) What's the hype about CDK5RAP2? *Cell. Mol. Life Sci.* **68,** 1719–1736
39. Choi, Y. K., Liu, P., Sze, S. K., Dai, C., and Qi, R. Z. (2010) CDK5RAP2 stimulates microtubule nucleation by the γ-tubulin ring complex. *J. Cell Biol.* **191,** 1089–1095
40. Hanafusa, H., Kedashiro, S., Tezuka, M., Funatsu, M., Usami, S., Toyoshima, F., and Matsumoto, K. (2015) PLK1-dependent activation of LRRK1 regulates spindle orientation by phosphorylating CDK5RAP2. *Nat. Cell Biol.* **17,** 1024–1035
41. Kim, S., and Rhee, K. (2014) Importance of the CEP215-pericentrin interaction for centrosome maturation during mitosis. *PLoS ONE* **9,** e87016
42. Jia, Y., Fong, K. W., Choi, Y. K., See, S. S., and Qi, R. Z. (2013) Dynamic recruitment of CDK5RAP2 to centrosomes requires its association with dynein. *PLoS ONE* **8,** e68523
43. Barr, A. R., Kilmartin, J. V., and Gergely, F. (2010) CDK5RAP2 functions in centrosome to spindle pole attachment and DNA damage response. *J. Cell Biol.* **189,** 23–39
44. Larocca, M. C., Shanks, R. A., Tian, L., Nelson, D. L., Stewart, D. M., and Goldenring, J. R. (2004) AKAP350 interaction with cdc42 interacting protein 4 at the Golgi apparatus. *Mol. Biol. Cell* **15,** 2771–2781
45. Graser, S., Stierhof, Y. D., and Nigg, E. A. (2007) Cep68 and Cep215 (Cdk5rap2) are required for centrosome cohesion. *J. Cell Sci.* **120,** 4321–4331
46. Bahe, S., Stierhof, Y. D., Wilkinson, C. J., Leiss, F., and Nigg, E. A. (2005) Rootletin forms centriole-associated filaments and functions in centrosome cohesion. *J. Cell Biol.* **171,** 27–33
47. Pagan, J. K., Marzio, A., Jones, M. J., Saraf, A., Jallepalli, P. V., Florens, L., Washburn, M. P., and Pagano, M. (2015) Degradation of Cep68 and PCNT cleavage mediate Cep215 removal from the PCM to allow centriole separation, disengagement and licensing. *Nat. Cell Biol.* **17,** 31–43
48. Guarguaglini, G., Duncan, P. I., Stierhof, Y. D., Holmström, T., Duensing, S., and Nigg, E. A. (2005) The forkhead-associated domain protein Cep170 interacts with Polo-like kinase 1 and serves as a marker for mature centrioles. *Mol. Biol. Cell* **16,** 1095–1107
49. Fry, A. M. (2015) Solving the centriole disengagement puzzle. *Nat. Cell Biol.* **17,** 3–5
50. Fang, G., Zhang, D., Yin, H., Zheng, L., Bi, X., and Yuan, L. (2014) Centlein mediates an interaction between C-Nap1 and Cep68 to maintain centrosome cohesion. *J. Cell Sci.* **127,** 1631–1639